A&A 402, L47–L54 (2003)
DOI: 10.1051/0004-6361:20030339

Astronomy & Astrophysics

Odin⋆ water mapping in the Orion KL region

A. O. H. Olofsson[1], G. Olofsson[2], Å. Hjalmarson[1], P. Bergman[1], J. H. Black[1], R. S. Booth[1], V. Buat[3], C. L. Curry[4], P. J. Encrenaz[5], E. Falgarone[6], P. Feldman[7], M. Fich[4], H. G. Florén[2], U. Frisk[8], M. Gerin[6], E. M. Gregersen[9], J. Harju[10], T. Hasegawa[11], L. E. B. Johansson[1], S. Kwok[11], B. Larsson[2], A. Lecacheux[12], T. Liljeström[13], R. Liseau[2], K. Mattila[10], G. F. Mitchell[14], H. L. Nordh[15], M. Olberg[1], H. Olofsson[2], L. Pagani[5], R. Plume[11], I. Ristorcelli[16], G. Rydbeck[1], Aa. Sandqvist[2], F. von Schéele[8], G. Serra[16,⋆⋆], N. F. Tothill[14], K. Volk[11], and C. D. Wilson[9]

[1] Onsala Space Observatory (OSO), 439 92 Onsala, Sweden
[2] Stockholm Observatory, SCFAB, Roslagstullsbacken 21, 106 91 Stockholm, Sweden
[3] Laboratoire d'Astronomie Spatiale, BP 8, 13376 Marseille Cedex 12, France
[4] Department of Physics, University of Waterloo, Waterloo, ON N2L 3G1, Canada
[5] LERMA & FRE 2460 du CNRS, Observatoire de Paris, 61 Av. de l'Observatoire, 75140 Paris, France
[6] LERMA & FRE 2460 du CNRS, École Normale Supérieure, 24 rue Lhomond, 75005 Paris, France
[7] NRC-HIA, Herzberg Institute of Astrophysics, 5071 West Saanich Road, Victoria, BC V9E 2E7, Canada
[8] Swedish Space Corporation, PO Box 4207, 171 04 Solna, Sweden
[9] Department of Physics and Astronomy, McMaster University, Hamilton, ON L8S 4M1, Canada
[10] Observatory, PO Box 14, University of Helsinki, 00014 Helsinki, Finland
[11] Department of Physics and Astronomy. University of Calgary, Calgary, ABT 2N 1N4, Canada
[12] LESIA, Observatoire de Paris, Section de Meudon, 5 place Jules Janssen, 92195 Meudon Cedex, France
[13] Metsähovi Radio Observatory, Helsinki University of Technology, Otakaari 5A, 02150 Espoo, Finland
[14] Department of Astronomy and Physics, Saint Mary's University, Halifax, NS B3H 3C3, Canada
[15] Swedish National Space Board, Box 4006, 171 04 Solna, Sweden
[16] CESR, 9 avenue du Colonel Roche, BP 4346, 31029 Toulouse, France

Received 3 December 2002 / Accepted 14 February 2003

Abstract. New results from water mapping observations of the Orion KL region using the submm/mm wave satellite Odin (2.1′ beam size at 557 GHz), are presented. The *ortho*-H_2O $J_{K+K-} = 1_{1,0} \rightarrow 1_{0,1}$ ground state transition was observed in a 7′ × 7′ rectangular grid with a spacing of 1′, while the same line of $H_2^{18}O$ was measured in two positions, Orion KL itself and 2′ south of Orion KL. In the main water species, the KL molecular outflow is largely resolved from the ambient cloud and it is found to have an extension of 60″–110″. The H_2O outflow profile exhibits a rather striking absorption-like asymmetry at the line centre. Self-absorption in the near (or "blue") part of the outflow (and possibly in foreground quiescent halo gas) is tentatively suggested to play a role here. We argue that the dominant part of the KL $H_2^{18}O$ outflow emission emanates from the compact (size ∼15″) low-velocity flow and here estimate an H_2O abundance of circa 10^{-5} compared to all H_2 in the flow – an order of magnitude below earlier estimates of the H_2O abundance in the shocked gas of the high-velocity flow. The narrow ambient cloud lines show weak velocity trends, both in the N-S and E-W directions. $H_2^{18}O$ is detected for the first time in the southern position at a level of ∼0.15 K and we here estimate an H_2O abundance of (1–8) $\times 10^{-8}$.

Key words. ISM: abundances – ISM: individual objects: Orion KL – ISM: molecules – submillimeter

1. Introduction

The Orion KL molecular outflow region, at a distance of only 500 pc, has been studied in great detail with a wide variety of instruments (cf. Melnick et al. 2000b; Wilson et al. 2001). There are strong indications that the compact HII source called I (Menten & Reid 1995) is the centre of the dynamical activity, being the central position for a dense group of H_2O and SiO masers (Gaume et al. 1998; Wright et al. 1995). Still, the compact luminous "Hot Core", as revealed by interferometric

Send offprint requests to: A. O. H. Olofsson,
e-mail: henrik@oso.chalmers.se

⋆ Odin is a Swedish-led satellite project funded jointly by the Swedish National Space Board (SNSB), the Canadian Space Agency (CSA), the National Technology Agency of Finland (Tekes), and the Centre National d'Études Spatiales (CNES, France). The Swedish Space Corporation (SSC) was the industrial prime contractor and is also responsible for the satellite operation.

⋆⋆ Deceased.

observations, is centred at least 500 AU away from source I (Wright et al. 1996; Vicente & Martín-Pintado 2002), leaving some doubts that source I is the power source for the Hot Core. Other compact molecular cores are found in the close vicinity of source I, like the "Compact Ridge" and the "Northern Cloud" (Wright et al. 1996). Mid-IR mapping reveals a number of bright, more or less pointlike sources (Gezari et al. 1998) in addition to the IR nebula named after its discoverers (Kleinmann & Low 1967). It is generally assumed that the mid-IR nebulosity is due to dust emission as the scattering efficiency of small grains is low at these wavelengths. On the other hand, the next brightest mid-IR source, Irc2 (Rieke et al. 1973), appears to be a reflection nebula, at least in view of the observed polarisation at 3.6 μm (Dougados et al. 1993). This source, traditionally identified as the dynamical centre, may well be powered by near- or mid-IR emission from source I. If so, source I must be heavily obscured in our line of sight (presumably by the Compact Ridge) and much less so in the direction of Irc2. The spatial distribution of the SiO $v=0$, $J=2\rightarrow1$ emission and the SiO $v=1$, $J=2\rightarrow1$ masers, together with the observed velocity patterns, suggest that source I is surrounded by a flared disc oriented in the SW-NE direction (Wright et al. 1995) allowing radiation to reach the two dense compact cores, Irc2 and the "hot core".

However, such a protostar with a disc seen more or less edge-on, should give rise to a well-behaved bipolar outflow in the SE-NW directions. Even though weak bipolar tendencies have been reported (H. Olofsson et al. 1982; Masson et al. 1987; Wilson et al. 2001), it is generally agreed that the outflow is viewed almost face-on and has a very wide opening angle. Seen at high spatial resolution, it is clear that much of the shock-excited high-velocity 2 μm H_2 emission is coming from numerous condensations (Sugai et al. 1995; Salas et al. 1999). Whether these condensations are accelerated by a strong wind (not yet observed), or are originating from the close environment of the protostar, is not clear. Recent proper motion observations of HH objects at large projected distances from their dynamical centres suggest an explosive event 1000 years ago (Doi et al. 2002). This might have been a powerful version of the FU Ori phenomenon.

In addition to exploring the dynamical properties of the Orion/KL outflow, much observational effort has been spent on the chemical aspects, due to the brightness of the source and the richness of its microwave spectrum (cf. Sutton et al. 1995). Most of the molecular emission comes from the molecular cores near the dynamical centre, and from the inner (lower velocity) expanding region called the "Plateau" source (named after the shapes of the emission lines, cf. Genzel & Stutzki 1989). The diameter of this expanding region is 15″–30″ (Masson et al. 1987; Pardo et al. 2001), while the extent of the shock-excited 2 μm H_2 emission and (post-shock) HCO^+ flow is larger than 1′ (Sugai et al. 1995; Salas et al. 1999; Olofsson et al. 1982; Vogel et al. 1984).

On a larger scale, the KL region is one of the centres of active star formation along the elongated "Extended Ridge" that makes up the OMC-1 GMC, which in turn is a prominent component of the Orion A molecular cloud. Comprehensive studies on the physical and chemical molecular structure of this region can be found in e.g. Castets et al. (1990), Dutrey et al. (1993), and Ungerechts et al. (1997). The HII region M42, powered by the Trapezium stars, is partly located in front of the KL region and the interfacing PDR region (the "Orion Bar", cf. Wilson et al. 2001; Larsson et al. 2003, in this issue) adds to the richness and complexity from a spectroscopic point of view.

In this Letter, we add further important clues to the Orion KL enigma, in the form of core region mapping observations at 1′ spacing of the *ortho*-H_2O and *ortho*-$H_2^{18}O$ ground state submm rotational lines, performed by Odin, a Swedish-led astronomy and aeronomy satellite observatory[1]. Odin was launched on 20 February 2001 by a Start-1 rocket, from Svobodny in eastern Russia (Nordh et al. 2003, in this issue).

2. Observations

The observing runs discussed here took place on 24 September 2001, 15/17 April 2002 (H_2O, $7'\times7'$ map, ∼15 h on-source integration time), and on 27 September, 15 October 2001 ($H_2^{18}O$, three positions, ∼20 h on-source).

Two different tunable submm receivers were used for the $J_{K_aK_c}=1_{1,0}\rightarrow1_{0,1}$ water lines ($H_2^{16}O$ at 556.936 GHz and $H_2^{18}O$ at 547.67644 GHz), having average SSB system temperatures of 3200 K and 3500 K, respectively.

The spectra were recorded with a hybrid autocorrelator spectrometer (AC) configured for a channel spacing of 0.5 MHz (working bandwidth 300 MHz), and an AOS (1 MHz resolution and ∼1.1 GHz bandwidth). A sky switching scheme was employed (5 or 10 s cycle), either looking at the main beam (1.1 m aperture, FWHM circular beam size ∼2.′1 at 557 GHz) or at one of the two available sky beams (of 4°size, ∼40° offset from the telescope axis), cf. Frisk et al. (2003), in this issue.

The pointing reconstruction uncertainty is very small (around 5″) in the large majority of the data. After correcting for absolute beam offsets using dedicated Jupiter observations close in time to our Orion measurements, we estimate that any residual disalignment between the two Orion maps is no larger than 10″. From the Jupiter data, we also find that our beam efficiency is close to 90% (cf. Hjalmarson et al. 2003, in this issue).

Data were calibrated using the standard chopper wheel method, switching between an internal hot load and the main beam (Olberg et al. 2003, in this issue).

Furthermore, the $H_2^{18}O$ data have been subtracted with calibrated off-source AOS measurements and a polynomial baseline, while the $H_2^{16}O$ map data (where the amount of line-free baseline region in the 300 MHz AC spectrometer band is limited at positions of broad emission) have merely been subtracted with one common sinusoidal fit (Fig. 1, lower right insert) applied to an average of the available spectra off source (together with peripheral parts of the map where the lines are narrow). We have benefitted in this procedure from the ability to cross check our results with the broad band AOS data from the complementary water receiver.

[1] http://www.snsb.se/eng_odin_intro.shtml

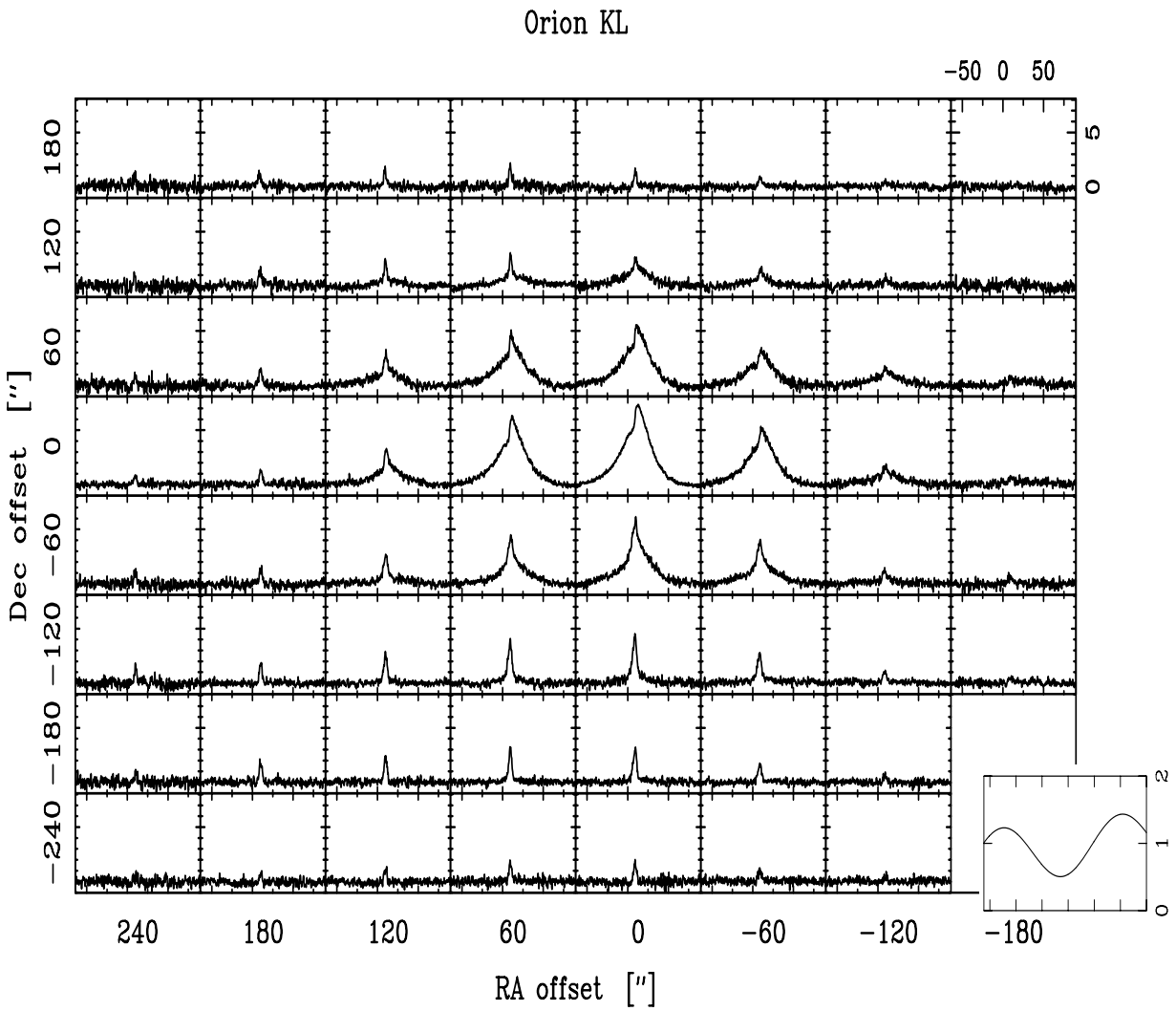

Fig. 1. The Odin 557 GHz H_2O map[2]. The increments of the velocity and intensity axes are given next to the top right spectrum. The map origin corresponds to J2000 coordinates $\alpha = 05^h35^m14\overset{s}{.}4$, $\delta = -05°22'30''$. Lower right insert: one of the two sinusoids subtracted from each scan in the two water map observations in order to compensate for a standing wave phenomenon. Note here the magnified intensity scale.

A general discussion about Odin's performance can be found in Hjalmarson et al. (2003), and a technical description of the spacecraft is given in Frisk et al. (2003).

3. Results and discussion

3.1. Data properties

3.1.1. H_2O

Figure 1 shows a position-averaged version of the entire *ortho*–H_2O spectra map. Individual scans were observed around grid points slightly different from those shown (due to systematic attitude reconstruction scatter, and to pointing model adjustments). In order to visualise the data, we have chosen to "regrid" the map so that it retains the nominal map spacing of 1′ and to centre the map at the Orion KL position. This method implies an additional spatial smearing so that the effective resolution becomes 130–140″. We emphasise that the original data set was used in the preliminary map analysis in Sect. 3.2.2. As briefly discussed at the end of this Letter, a more detailed analysis based on a deconvolved Odin water map will appear in a subsequent A&A paper.

As is evident, we detect water emission at nearly all map points, although the velocity integrated flux density is heavily dominated by the KL outflow source, as expected from the lower resolution map by Snell et al. (2000), obtained using the SWAS space telescope (3.3′ × 4.5′ beam, cf. Melnick et al. 2000b).

There is pronounced velocity structure present, both in the Extended Ridge/Bar narrow line emission, and in the KL outflow high velocity wings. The E-W trend across the Extended Ridge into the Bar is illustrated in Fig. 2 by a sequence of spectra at −2′ DEC offset, and the S-N structure across KL is shown in a velocity-declination diagram (Fig. 3). In the former figure, water emission is indeed seen at Orion Bar velocities (∼10.5 km s^{-1}, Wilson et al. 2001), where Odin also has

[2] All figure intensity axes are given in units of antenna temperature if not stated otherwise.

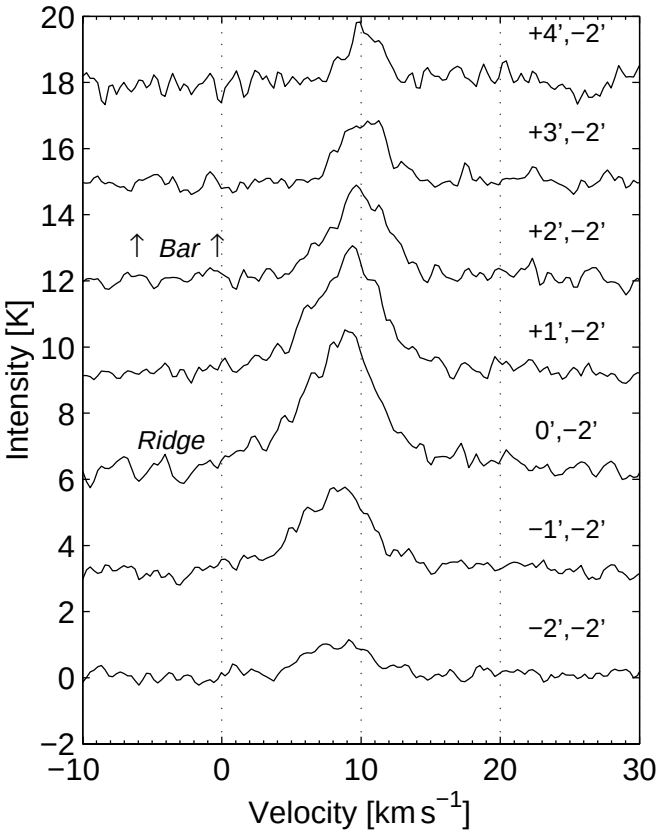

Fig. 2. H_2O spectra[2] from Fig. 1 along a line of constant declination (2′ south of Orion KL). The sequence goes from west to east in steps of 1′ from bottom to top (the offsets are given at the right hand side).

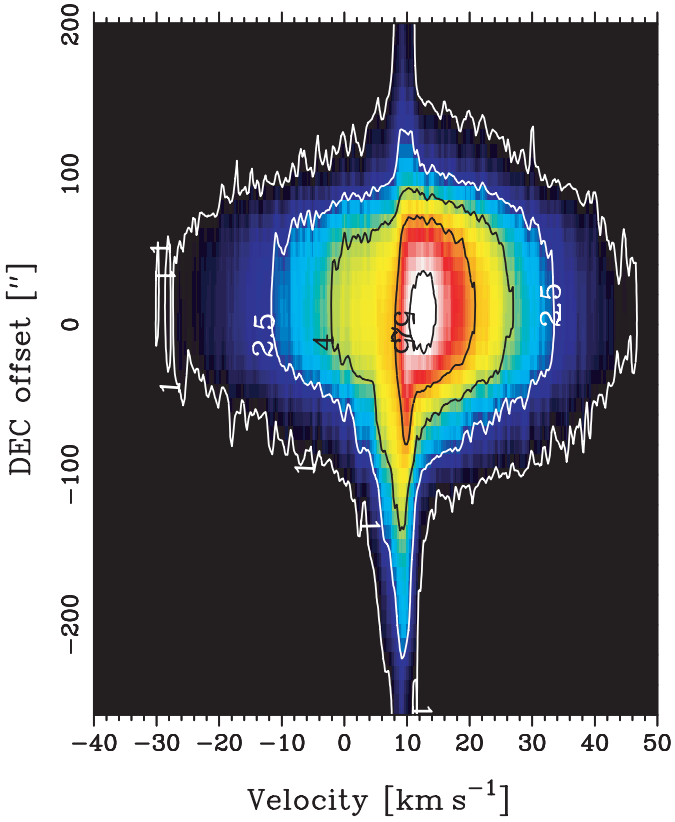

Fig. 3. H_2O declination-velocity diagram through Orion KL. The colour coding goes from black (≤1 K), to white (≥7 K). The contours[2] start at 1 K and are incremented with 1.5 K.

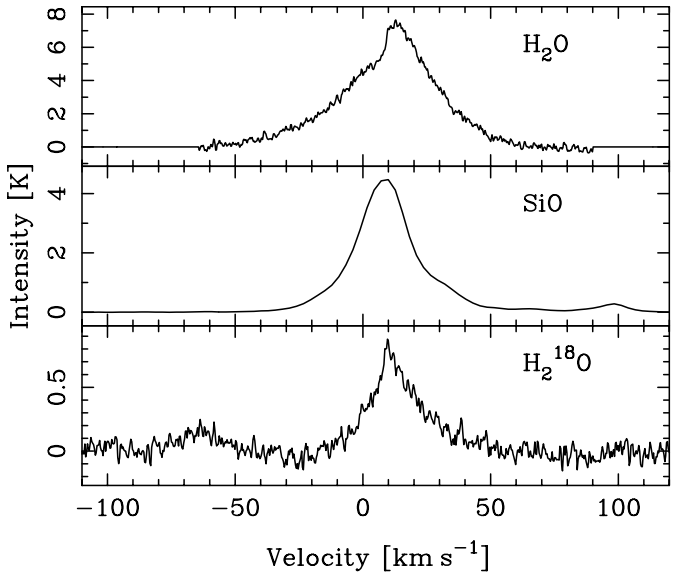

Fig. 4. From top to bottom: H_2O (Odin beam 2.1′), SiO (Onsala; beam size 0.7′), and (Odin) $H_2^{18}O$ (accompanied by an SO_2 emission line at ∼–60 km s^{-1}, see text). Note the different vertical scales[2].

detected NH_3 (Larsson et al. 2003). Apart from the outflow appearance in Fig. 3 (discussed further below), the emission centroids shifts from ∼8–9 km s^{-1} in the south to ∼9–10 km s^{-1} in the north, in agreement with the two cloud components at these velocities previously detected by e.g. Rydbeck et al. (1981) and Friberg (1984).

The Odin Orion KL water spectrum is shown separately in Fig. 4, together with a $v=0$, $J=2\rightarrow1$ spectrum of SiO (observed with a 43″ beam using the Onsala 20 m telescope), and the Odin $H_2^{18}O$ spectrum (described further below). Compared with the corresponding water spectrum observed by SWAS (Melnick et al. 2000a), the Odin spectrum clearly has resolved out the outflow emission better from the ambient cloud narrow emission. In fact, a convolution of our Odin H_2O map (Fig. 1) to the SWAS resolution results in an H_2O spectrum almost identical to the one observed by SWAS (as demonstrated by Hjalmarson et al. 2003). The high velocity portions of the H_2O and SiO profiles are very similar, suggesting an outflow/shock origin of the water line as well. However, an important difference between the two is the water central asymmetry – the bluewards absorption-like feature (further discussed in Sect. 3.2). This peculiarity (which is confirmed by data from the complementary water frontend/AOS backend system; see Fig. 1 of Hjalmarson et al. 2003) also seem to be slightly more emphasised ∼1′ northwards from the KL position.

3.1.2. $H_2^{18}O$

Our Orion KL $H_2^{18}O$ AOS spectrum (Fig. 4) – at first reduced in the manner described in Sect. 2 – was additionally treated for a residual sinusoidal-like interference, a measure that may formally underestimate the strength by ≤4%. Since the baseline

in the AOS spectrum extends far beyond what is shown here (and is now largely flat), we find no reason to believe that the process has distorted the line shape further. There are a few features immediately worth pointing out (some of which are discussed more in Sect. 3.2):

– The best Gaussian fit to the spectrum is made when the central, very peaked part, is excluded. Such a fit gives a line width of ~27 km s^{-1} similar to that observed by SWAS (see Hjalmarson et al. 2003, for a direct Odin/SWAS comparison). The strength of the central narrow excess emission (~0.25 K) is fairly consistent with our $H_2^{18}O$ detection in the southern position (see below). Therefore, this component could be interpreted as a contribution from the Extended Ridge.
– The other spectral line seen about 70 km s^{-1} bluewards of the $H_2^{18}O$ line, is the high energy ($E_l \approx 450$ K) SO_2 $J_{K_+K_-} = 28_{6,22} \rightarrow 28_{5,23}$ transition at 547.80222 GHz. This line is also visible in the SWAS spectrum, giving us (since the Odin/SWAS beam sizes differ) an excellent opportunity to estimate relative source sizes as seen in $H_2^{18}O$ and SO_2 emission (see Hjalmarson et al. 2003).
– In the red and blue wings, respectively, there are two marginally evident features: low-level emission at high velocities ("shock emission", similar to H_2O and SiO), and a possible absorption-like broad dip in the blue wing that approaches the SO_2 line.

Towards the southern position, we have with a high level of confidence detected $H_2^{18}O$ emission likely originating in the Extended Ridge (Fig. 5). Integration time weighted averages of the two different observations (27 September and 15 October 2001, Fig. 5a) were subtracted with 5th order baselines fitted to the baseline regions indicated by the boxes in Fig. 5b. The final average was then obtained using baseline RMS weighting. The integrated emission in the velocity interval 1–15 km s^{-1} is 0.7 ± 0.07 K km s^{-1}. Our main arguments for this detection can be summarised as follows:

(i) The line is evident in both of our two observation sessions although the later observation (15 October 2001) has a higher baseline noise due to a shorter net integration time. On the other hand, the October 15th observation was performed measuring a signal-free reference spectrum every 5 min, allowing us to compensate for variability in the intrinsic baseline pattern produced by the receiver system (cf. Hjalmarson et al. 2003).
(ii) The emission feature peaks at similar LSR velocities for the two observations (~8 km s^{-1}). This is also markedly different from the peak $H_2^{18}O$ velocity in the Orion KL position (Fig. 4), allowing us to exclude the possibility that narrow emission from the KL position has been blended into the southern position observation.
(iii) As an additional test, we also subtracted the on source data set with an average of itself which was uncompensated for the periodical velocity change due to satellite motion, so that a narrow astronomical line would be substantially smeared and diminished. This is *not* the case for e.g. a channel stable spike produced internally in the receiver system. After the test subtraction, there was still a line above the noise level signifying an astronomical origin of the line.

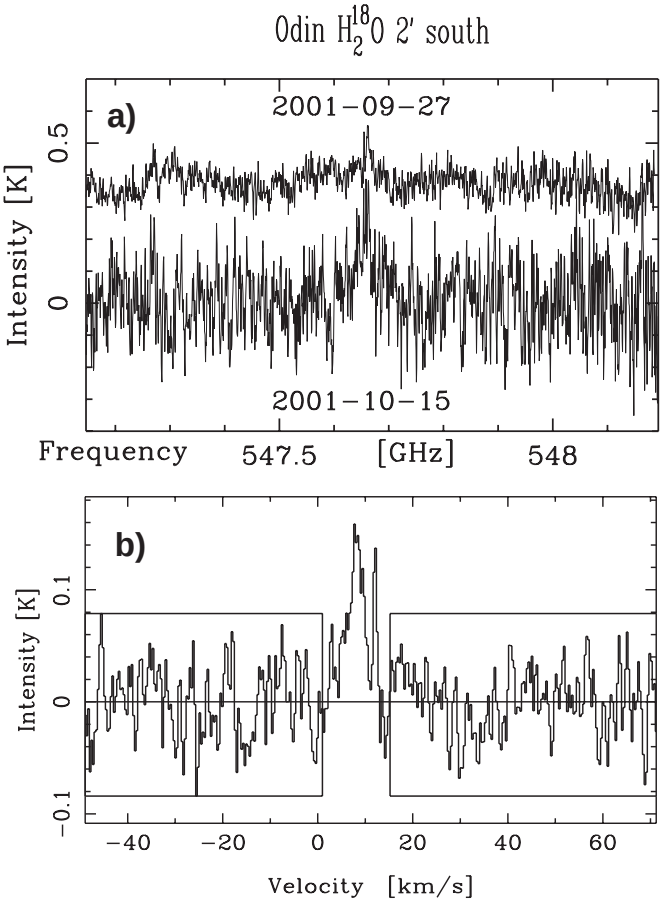

Fig. 5. $H_2^{18}O$ towards 2′ south of Orion KL[2]. **a)** The two separate sky-switched spectra (observed at the dates indicated in the figure) with additional reference positions subtracted. The upper spectrum has been offset upwards with 0.2 K. **b)** The same observations clipped and RMS averaged after polynomial baseline subtractions (see text for further details).

In view of the rather low SWAS limit for this line (Snell et al. 2000, centred 3′.2 south of Orion KL), we infer that the $H_2^{18}O$ source size should be compact, which may be expected if the emission primarily comes from a previously detected warm massive clump in the Orion ridge (NH_3: Source 6 in Batrla et al. 1983; CS condensation 4 in the high resolution map of Mundy et al. 1988). Since a detection of an ambient cloud $H_2^{18}O$ line is very important for a reliable determination of the water abundance, we aim at verifying this probable detection, and also at observing additional ambient cloud positions, in the near future.

3.2. Interpretation

3.2.1. Line shapes

To illuminate similarities and differences in our H_2O, $H_2^{18}O$, and SiO spectra, we show them together in Fig. 6 scaled so that their red line wings overlap. We note first that all three lines

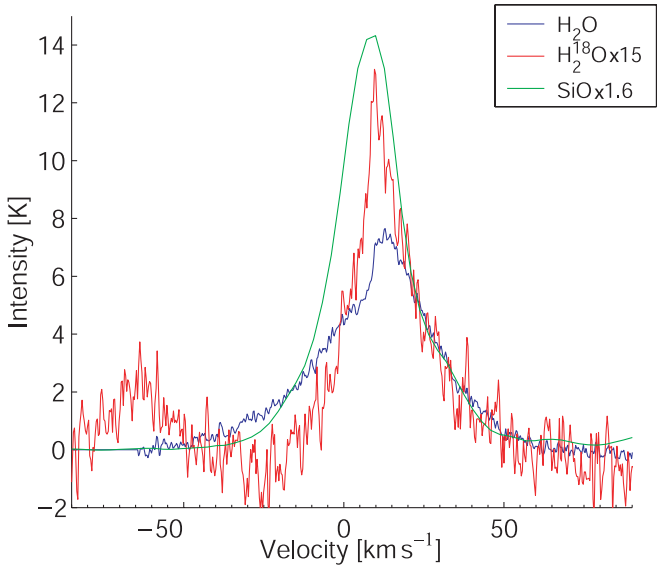

Fig. 6. The spectra of Fig. 4 scaled[2] according to the legend. Note that the SiO profile was corrected for the OSO 20 m beam efficiency before scaling.

seem to lack evidence for emission features characteristic for the Hot Core or the Compact Ridge.

The H_2O line has, compared to the SiO line, a central asymmetry that takes the form of an emission deficiency from the line centre into the blue wing of the water line. We tentatively consider the H_2O profile to show evidence of broad outflow self-absorption, consistent with what is sometimes seen in optically thick lines from expanding regions such as circumstellar shells (CO; Crosas & Menten 1997), and cometary comae (Odin H_2O; Lecacheux et al. 2003, in this issue). The steep change in the proposed H_2O KL self-absorption occurs at the systemic velocity of the ambient cloud (8 to 10 km s^{-1}). A similar behaviour – narrow absorptions at systemic velocities – is found to an even larger extent in most of the outflow sources observed by Odin and SWAS. We tentatively suggest that such water self-absorption, occuring in the line-of-sight lower-density outer layer of the quiescent cloud component, is an intrinsic radiative transfer property of water in warm GMC cores.

In the case of $H_2^{18}O$, there is an apparent shortage of emission compared to SiO out to a very low velocity (∼–30 km s^{-1}), possibly below the $H_2^{18}O$ baseline. If real (although currently hard to reconcile in view of our KL H_2O spectrum), the necessary continuum that is absorbed should come from the Hot Core and/or the Compact Ridge which are located behind the blue – or near – part of the outflow.

Another possibility is that the narrower width of the $H_2^{18}O$ line indicates that we see a different kinematical component in this species. A comparison then can be made with the submillimetre HDO lines observed by Pardo et al. (2001) which have similar widths and centre velocities. If the emission from these two molecules does indeed originate in the same gas, then the $H_2^{18}O$ profile is probably dominated by emission from the inner part of the outflow (low-velocity flow, or the "Plateau"), although the apparant presence of a red high velocity wing (which HDO clearly lacks) may indicate a minor contribution from the shocked gas (the proportions being determined by the optical depths involved). We will examine this interesting alternative more quantitatively in Sect. 3.2.3.

3.2.2. Source size estimates

An important clue to the interpretation of the water outflow/shock emission is the size and position of the source. Using the integrated intensity across the whole band (excluding only the very central part), we find that the peak is located 10″ north of our map centre. This location of the outflow centre is identical to the one determined by high resolution ground based observations (cf. Wilson et al. 2001). To estimate the source size, we have used three methods: i), a 2D Gaussian fit to the map integrated intensity corrected for the beam response, ii), a preliminary deconvolution of the integrated intensities in the red and blue line wings, and iii), through comparing the centre KL water spectra of Odin and SWAS (Hjalmarson et al. 2003). The Gaussian sizes all fall within the range 60″–110″.

In contrast to H_2O, Hjalmarson et al. concluded, through a direct Odin/SWAS comparison, that the $H_2^{18}O$ source size is pointlike in the Odin beam. Governed by the similarities between the $H_2^{18}O$ and HDO spectra (see Sect. 3.2.1), we will hereafter assume that the $H_2^{18}O$ sources size is 15″, i.e., equal to extent of the submillimetre HDO emission from the low-velocity Plateau (Pardo et al. 2001).

The H_2O source size in the southern position (2′ south of KL) is simply taken to be larger than the Odin beam since the narrow line emission is obviously extended (cf. Fig. 1).

3.2.3. Water content

We will herein attempt a very simple analysis and bring forth a few basic comments in connection with our observational results. A detailed treatment is planned to appear in an A&A paper in the near future, the prospects of which are discussed at the end of this Letter.

To derive the water content, we have used the optically thin LTE approximation applied to the $H_2^{18}O$ line. In this limit, the expression for the water column density takes the form:

$$N(\mathrm{H_2O}) = \alpha(T)\, R\, \eta_{\mathrm{bf}}^{-1}\, I_{\mathrm{mb}}\left(\mathrm{H_2^{18}O}\right) \quad (1)$$

where $\alpha(T)$ is dependent on the population distribution temperature T, and η_{bf} is the beam filling factor. We have assumed an *ortho–para* ratio of 3 and $N(H_2O)$ is thus an estimate of the total water column density. R is the $^{16}O/^{18}O$ isotope ratio here taken to be ∼500 (Wilson & Rood 1994). The integrated main beam brightness temperatures, I_{mb}, together with H_2O column densities are listed in Table 1.

Using an η_{bf} corresponding to our adopted $H_2^{18}O$ source size of 15″, a rotation temperature T = 72 K ($\alpha(72)$ = 5.86×10^{11} s K^{-1} km^{-1} cm^{-2} in Eq. (1)) as found by Wright et al. (2000), we obtain $N(H_2O) = 4 \times 10^{17}$ cm^{-2}. This value is about a factor of four lower than the column density obtained from pure rotational H_2O lines in the 25–45 μm band

Table 1. Integrated intensities, column densities, and abundances.

Position rel. to KL	I_{mb} (K km s^{-1})		$N(H_2O)$[a]	$X(H_2O)$[a]
	H_2O	$H_2^{18}O$	(cm^{-2})	
0′, 0′	323	18.6	4×10^{17}[b]	1×10^{-4}[c] / 8×10^{-6}[d]
0′, –2′	24.0	0.78	9×10^{13}	10^{-8}[e]

[a] Using the optically thin LTE approximation with $H_2^{18}O$ and T = 72 K and 25 K for KL and 2′S, respectively.
[b] Assuming an $H_2^{18}O$ Gaussian source size of 15″.
[c] For $N(H_2) = 3\times10^{21}$ cm^{-2} (shocked outflow component).
[d] For $N(H_2) = 5\times10^{22}$ cm^{-2} (total H_2 column through outflow).
[e] For $N(H_2) = 10^{22}$ cm^{-2} .

(Wright et al. 2000). When estimating the water abundance, $X(H_2O) = N(H_2O)/N(H_2)$, it is not obvious which $N(H_2)$ to use. For instance, if we adopt the H_2 column density of $\sim3\times10^{21}$ cm^{-2} estimated by Watson et al. (1985) from observations of far-infrared rotational CO lines, we obtain a water abundance of 1×10^{-4}. Alternatively, if we assume that the $H_2^{18}O$ gas is essentially the same component as seen in HDO, we instead find a Plateau water abundance of 8×10^{-6} (now using the *total* outflow H_2 column density of about 5×10^{22} cm^{-2} from Masson et al. 1988), which is more than an order of magnitude lower than our previous estimate. Both our estimates are listed in Table 1. Previous observations of broad water line components have all resulted in high abundances, e.g. (2–5) $\times10^{-4}$ (Wright et al. 2000, ISO mid-IR absorption lines), 5×10^{-4} (Harwit et al. 1998, ISO far-IR emission lines), and 3.5×10^{-4} (Melnick et al. 2000a, SWAS sub-mm emission line). As advocated by these authors, such high abundances are expected in shock-heated gas (cf. Kaufman & Neufeld 1996). Our water abundance may be underestimated in case the $H_2^{18}O$ line is optically thick in the Plateau. From the $H_2^{18}O$ column density and the observed line width, we find $\tau(H_2^{18}O) \approx 0.9$ for T = 72 K. This optical depth corresponds to an expected peak antenna temperature of about 0.5 K for a 15″ source size, i.e., consistent with the observed peak antenna temperature of 0.8 K. An optical depth of 0.9 implies an increase of our deduced water column density, and hence our water abundances, by a factor of ∼1.5.

Pardo et al. (2001) argue that the gas phase water in the low-velocity Plateau is more likely the result of evaporation of icy grain mantles by radiative heating (in turn explaining their high HDO abundance). Hence, we find no obvious contradiction in suggesting that the Plateau water abundance may be smaller than the high value found in the post-shock gas. It is also worth noting that the Plateau column densities of HDO by Olofsson (1984) and Pardo et al., in combination with the H_2O column density found here, would imply a high degree of deuteration ($HDO/H_2O \sim 0.025$–0.1) in agreement with earlier findings for other deuterated molecules in Orion KL sources (Charnley et al. 1997; Mauersberger et al. 1988; Roberts et al. 2002).

The $H_2O/H_2^{18}O$ line ratio of emission in the red wings (the only part of the spectral range where the profiles look similar, see Fig. 6) is about 15, indicative of $\tau(H_2O) \gg 1$. Using the estimated size of 60″ for H_2O and the observed peak antenna temperature (8.1 K), we then find that the excitation temperature (for thermal emission) must be ∼56 K. This is close to the H_2O rotation temperature of 72 K (Wright et al. 2000). However, should the excitation temperature be substantially higher, e.g. ∼150 K (González-Alfonso et al. 2002), we need to introduce an additional source filling factor of about 0.4, as could be the case if a considerable part of the emission arises in small, dense, optically thick post-shock clumps. Such a filamentary and clumpy structure is seen over a ∼1′ region in H_2 $v=1\rightarrow0\,S(1)$ maps by Salas et al. (1999)[3]. Should the H_2O profile suffer strongly from self-absorption (see Sect. 3.2.1), a higher excitation temperature is indeed required.

In the southern position (2′ south of KL), we again employ the optically thin LTE approximation to estimate an ambient cloud water abundance and note that the peak brightness temperature ratio is $T_{mb}^{peak}(H_2O)/T_{mb}^{peak}(H_2^{18}O) = 24 \gg 1$, confirming that the $H_2^{18}O$ line is optically thin. For an LTE temperature of 25 K ($\alpha(25) = 2.38\times10^{11}$ s K^{-1} km^{-1} cm^{-2}) we obtain $N(H_2O) = 9\times10^{13}$ cm^{-2}. Using an H_2 column density of $\approx10^{22}$ cm^{-2} (Dutrey et al. 1993; Goldsmith et al. 1997), we find $X(H_2O) = 1\times10^{-8}$. This low value may be considered a lower limit since (as suggested in Sect. 3.1) the $H_2^{18}O$ beam filling factor may be as low as 10–15% judging from the clump size observed by Mundy et al. (1988). As a comparison, Snell et al. (2000) have demonstrated a method using the H_2O line itself to arrive at an abundance, provided that the line is optically thick and arising in strongly subthermal conditions. In the 2′S position, $\tau(H_2O)$ is estimated to be $500/24 = 21 \gg 1$. If we use the integrated intensity of our narrow component H_2O line from Table 1 together with the Eq. (2) of Snell et al. (here corrected for an *ortho–para* ratio of 3) valid for a kinetic temperature of 40 K and assume an H_2 density of 10^6 cm^{-3} and the same H_2 column density as before (10^{22} cm^{-2}), we instead arrive at a water abundance of $X(H_2O) = 8\times10^{-8}$.

Both our results are inconsistent with the high water abundance ($\lesssim10^{-5}$) estimated for gas adjascent to (but outside) the KL centre of activity by Cernicharo et al. (1994) using the 183 GHz water maser line. At present time, we concur with the opinion of Snell et al. that the maser line, which originates from energy levels near 200 K, must trace a denser and warmer gas component.

On the whole and at this stage, it appears that unequivocal estimates of the water abundances remain elusive, but the current work will be continued in a forthcoming paper where we aim at including all Orion water mapping data at our disposal (from past and future observations, including spectra from both Odin water receivers), in combination with new $H_2^{18}O$ and $H_2^{17}O$ observations. This will make feasable a more elaborate analysis and modelling, particularly in view of our ambition to produce a deconvolved water data cube (using the MEM-algorithm) that may reveal further details on, e.g., the Orion KL H_2O outflow absorption reported on above.

Acknowledgements. Generous financial support from the Research Councils and Space Agencies in Canada, Finland, France and Sweden

[3] See also www: http://subarutelescope.org/Science/press_release/9901/OrionKL_300.jpg

is gratefully acknowledged. We also want to thank the referee for constructive criticism which has strengthened our presentaion.

References

Batrla, W., Wilson, T. L., Bastien, P., et al. 1983, A&A, 128, 279
Castets, A., Duvert, G., Dutrey, A., et al. 1990, A&A, 234, 469
Cernicharo, J., González-Alfonso, E., Alcolea, J., Bachiller, R., & John, D. 1994, ApJ, 432, L59
Charnley, S. B., Tielens, A. G. G. M., & Rodgers, S. D. 1997, ApJ, 482, 203
Crosas, M., & Menten, K. M. 1997, ApJ, 483, 913
Doi, T., O'Dell, C. R., & Hartigan, P. 2002, AJ, 124, 445
Dougados, C., Lena, P., Ridgway, S. T., et al. 1993, ApJ, 406, 112
Dutrey, A., Duvert, G., Castets, A., et al. 1993, A&A, 270, 468
Friberg, P. 1984, A&A, 132, 265
Frisk, U., Hagström, M., Ala-Laurinaho, J., et al. 2003, A&A, 402, L27
Gaume, R. A., Wilson, T. L., Vrba, F. J., et al. 1998, ApJ, 493, 940
Genzel, R., & Stutzki, J. 1989, ARA&A, 27, 41
Gezari, D. Y., Backman, D. E., & Werner, M. W. 1998, ApJ, 509, 283
Goldsmith, P. F., Bergin, E. A., & Lis, D. C. 1997, ApJ, 491, 615
González-Alfonso, E., Wright, C. M., Cernicharo, J., et al. 2002, A&A, 386, 1074
Harwit, M., Neufeld, D. A., Melnick, G. J., & Kaufman, M. J. 1998, ApJ, 497, L105
Hjalmarson, Å, Frisk, U., Olberg, M., et al. 2003, A&A, 402, L39
Kleinmann, D. E., & Low, F. J. 1967, ApJ, 149, L1
Larsson, B., Liseau, R., Bergman, P., et al. 2003, A&A, 402, L69
Lecacheux, A., Biver, N., Crovisier, D., et al. 2003, A&A, 402, L55
Kaufman, M. J., & Neufeld, D. A. 1996, ApJ, 456, 611
Masson, C. R., Lo, K. Y., Phillips, T. G., et al. 1987, ApJ, 319, 446
Mauersberger, R., Henkel, C., Jacq, T., & Walmsley, C. M. 1988, A&A, 194, 1
Melnick, G. J., Ashby, M. L. N., Plume, R., et al. 2000a, ApJ, 539, L87
Melnick, G. J., Stauffer, J. R., Ashby, M. L. N., et al. 2000b, ApJ, 539, L77
Menten, K. M., & Reid, M. J. 1995, ApJ, 445, L157
Mundy, L. G., Cornwell, T. J., Masson, C. R., et al. 1988, ApJ, 325, 382
Nordh, H. L., von Schéele, F., Frisk, U., et al. 2003, A&A, 402, L21
Olberg, M., Frisk, U., Lecacheux, A., et al. 2003, A&A, 402, L35
Olofsson, H. 1984, A&A, 134, 36
Olofsson, H., Elldér, J., Hjalmarson, Å, & Rydbeck, G. 1982, A&A, 113, L18
Pardo, R. P., Cernicharo, J., Herpin, F., et al. 2001, ApJ, 562, 799
Rieke, G. H., Low, F. J., & Kleinmann, D. E. 1973, ApJ, 186, L7
Roberts, H., Fuller, G. A., Millar, T. J., Hatchell, J., & Buckle, J. V. 2002, A&A, 381, 1026
Rydbeck, O. E. H., Hjalmarson, Å, Rydbeck, G., et al. 1981, ApJ, 243, L41
Salas, L., Rosando, M., Cruz-Gonzalez, I., et al. 1999, ApJ, 511, 822
Snell, R. L., Howe, J. E., Ashby, et al. 2000, ApJ, 539, L93
Sugai, H., Kawabata, H., Usuda, T., et al. 1995, ApJ, 442, 674
Sutton, E. C., Peng, R., Danchi, W. C., et al. 1995, ApJS, 97, 455
Ungerechts, H., Bergin, E. A., Goldsmith, P. F., et al. 1997, ApJ, 482, 245
Vicente, P. de, & Martín-Pintado, J. 2002, ApJ, 574, L163
Vogel, S. N., Wright, M. C. H., Plambeck, R. L., & Welch, W. J. 1984, ApJ, 283, 655
Watson, D. M., Genzel, R., Townes, C. H., & Storey, J. W. V. 1985, ApJ, 298, 316
Wilson, T. L., Muders, D., Kramer, C., & Henkel, C. 2001, ApJ, 557, 240
Wilson, T. L., & Rood, R. T. 1994, A&AR, 32, 191
Wright, M. C. H., Plambeck, R. L., Mundy, L. G., & Looney, L. W. 1995, ApJ, 455, L185
Wright, M. C. H., Plambeck, R. L., & Wilner, D. J. 1996, ApJ, 469, 216
Wright, C. M., van Dishoeck, E. F., Black, J. H., et al. 2000, A&A, 358, 689